Slovak Geol. Mag., 20, 1 (2020), 85 – 98

4. Use of Geostatistical Simulation in Reservoir Thermodynamics Assessment and Interpretation at the Ďurkov Hydrogeothermal Structure, Slovakia

Vizi Ladislav, Fričovský Branislav, Zlocha Marian & Surový Martin

State Geological Institute of Dionýz Štúr, Mlynská dolina, Bratislava, Slovak Republic, ladislav.vizi@geology.sk

Abstract: Geothermal energy in Slovakia is under a systematic research since 70's of the last Century. Out of 27 identified prospective geothermal fields within a territory of the Western Carpathians, the Ďurkov hydrogeothermal structure in the Košice Depression is repeatedly accented as of the most enormous potential for a heat (and in some, rather wishful, plans for power) production. Unlike a conventional evaluation of thermal potential and temperature, this study aims at description of the reservoir under an exergy concept; quantifying reservoir enthalpy, exergy and specific exergy index based on geostatistical modelling prior classifying a system according to a thermodynamic quality.
Geostatistical simulations have become very popular in different areas of spatial modelling for spatial simulation of properties, geometries or heterogeneities. The geostatistical approach is supportive to quantification and interpretation necessary to understand for reservoir engineering and construction of reservoir prediction and response models. Turning band method of simulation was used to create multiple realisations of the convection indicators within the reservoir body due to evident non-stationary behaviour, mainly in vertical direction, which made it impossible to use Gaussian type model. Non-conditional simulations were tested conditioned by universal kriging using modelled variograms of global trend residuals with respective drift functions for each studied variable. The risk volumetric curves were derived from final numerical models and probable reservoir volumes above different boundary conditions (cut-offs) were calculated and visualised. Based on numerical models, reservoir enthalpy greater than 800 $kJ.kg^{-1}$ has been identified in deeper parts of a system with very small proportion of specific exergy index above 0.2. Thermodynamic data, and models based on them, show the resource is rather suitable for a large-scale heat (district heating) production – supply.
Key words: thermodynamic quality, reservoir enthalpy, geostatistics, simulation, volumetrics

4.1 Foreword

The Slovak Republic is a low atmosphere harmful substances (AHS) country with mean yearly emissions of 25 % below a ratified level. Although, national economy is still fossil-fuels oriented. Indeed, renewables contribute only 23 % on domestic electricity and 19 % on domestic heat primary energy consumption. By a contrast, onset of systematic research and development of geothermal energy dates back to the 70's of the last Century, progressively increasing a number of geothermal installations in a direct-use from 43 MWt in 1980 (Franko et al., 1990) to 149 MWt in 2015, not including heat pumps (Fendek & Fendeková, 2015). Recent global environmental constraints prompt, however, the country towards renewables. With 27 geothermal water bodies covering roughly 40 % of the country identified (Fendek & Fendeková, 2010), the geothermal energy appears of a significant potential, assumed app. 6,500 MWt in probable reserves.

The Ďurkov hydrogeothermal structure has been recognized the most prospective system amongst the all (e.g. Vranovská et al., 2000). Even several plans on district heating individual (e.g. Halás et al., 1999) or binary geothermal power plants bound (Kukurugyová et al., 2015) exist already, a conceptual, engineering approach to analyze the geothermal resource is still missing. Preliminary studies based on a borehole data classified the structure as of moderate-low exergy (Fričovský et al., 2016a, b). This paper presents a first insight into local reservoir thermodynamics and thermodynamic quality mapping.

4.2 Background

4.2.1 General consideration

Hydrogeological conditions triggering evolution of geothermal resources in Slovakia owe to lateral extension and vertical position of prospective Middle Triassic carbonates organized in multiple superpositioned nappes, resultant to Alpine tectonics; and Neogene Germanic-type neotectonics, forming deep sedimentary basins associating a resource with sands and sandstones in major (Franko & Melioris, 1999). Heat flux and accumulation outlines as consequent to different structure and depths of neotectonic blocks, overall crustal thickness and non-uniform mantle propagation, seating and depth of major crustal faults; and spatial distribution of Neogene – Early Pleistocene neovolcanism (Fendek et al., 1999). Still, geothermal plays in the Western Carpathians (Slovakia) are conduction-dominated, orogenic belt-type (Moeck, 2014).

Two different regions of geothermic activity are distinguished within the Western Carpathians. Intramountain depressions show rather low to moderate heat flux density (q = 60 – 90 $mW.m^{-2}$). This increases within Neogene deep sedimentary basins towards q = 90 – 120 $mW.m^{-2}$ (Franko & Melioris, 1999), classified moderate-high to high in local conditions. Amongst the latter is the Košice Depression (Fig. 4.1), terminated along Neogene volcanic range of the Slanské vrchy Mts. to east and a core-mountain massif of the Slovenské Rudohorie Mts. to the west (e.g. Vranovská et al., 2015).

4.2.2 Site description

The Ďurkov hydrogeothermal structure (DDHS) represents a depressed morphostructure of Mesozoic carbonates beneath, in vast majority, Neogene sedimentary basin fill in the western part of the Košice Depression. To the west, the structure terminates along a N-S trended fault zone parallel with the line connecting towns of Vyšný Čaj – Olšovany – Ďurďošík – Trsťany. Eastern margin corresponds with deep extension of the Neogene volcanites. A northern limit corresponds to the tectonic contact with the pre-Tertiary Bidovce Depression, whilst to the south, the system is delineated arbitrary to the uplifting blocks of Mesozoic carbonates along a Ruskov – Vyšný Čaj line (Fig. 4.1).

4.2.3 Deep geological structure

The Košice Depression as a neotectonic morpho-structure is resultant to the Neogene Germanic-type tectonics. In general, Quaternary exclusively terrestrial accumulations, Neogene sedimentary to minor volcanosedimentary formations and Mesozoic carbonates form a relevant deep geological structure. A crystalline beneath has not been subjected to a study yet. Obviously, the Quaternary accumulations (fluvial, proluvial and deluvial forms) are only several meters thick; thus, are usually neglected in vertical and horizontal extension. A thickness of the Neogene profile reaches up to 2,000 – 3,000 m within the structure. Atop, Sarmatian clays with rare rhyolite and andesite volcanoclastics are 200 – 1,000 m thick (Vranovská et al., 1999a). Beneath, carbonate sandy clays alternating sparsely with tuffites form up to 1,500 m thick Badenian part of the profile. Carbonate claystones with minor sandstones and basal brecciated conglomerates represent a bottom 400 – 600 m thick base of the Neogene succession (Vranovská et al., 2015).

Middle Triassic dolomites represent an analogue to the Krížna Nappe series of the Western Carpathians. Because of the tectonic dissection of the Košice Depression, a thickness of the Mesozoic profile varies between 200 – 2,000 m (Vranovská et al., 1999a), increasing pseudo-axially in the NW-SE and SW-NE direction. It is generally assumed that the greatest thickness corresponds to the major depression of the DDHS in the Ďurkov town area. However, the entire structure is dissected into several elevated and depressed blocks of the Mesozoic carbonates beneath the Neogene sedimentary cover along multiple faults; i.e. those of N-S and SW-NE trend in major.

A geochemical modelling conducted to explain high arsenic concentrations (cAs = 19 – 36 mg.l^{-1}) in Na-Cl type geothermal water associated with the DDHS (TDS = 20,000 – 30,000 mg.l^{-1}) has proven the system as hydrogeologically closed (Bodiš & Vranovská, 2012; Vranovská et al., 2015). A lack of natural reservoir recharge is amongst the most pronounced in considering of closed-loop systems at the site.

4.3 Methodology and approach

Under theoretical considerations, renewability of a geothermal resource at natural (initial, reservoir, etc.) conditions can be attributed to the closed thermodynamic

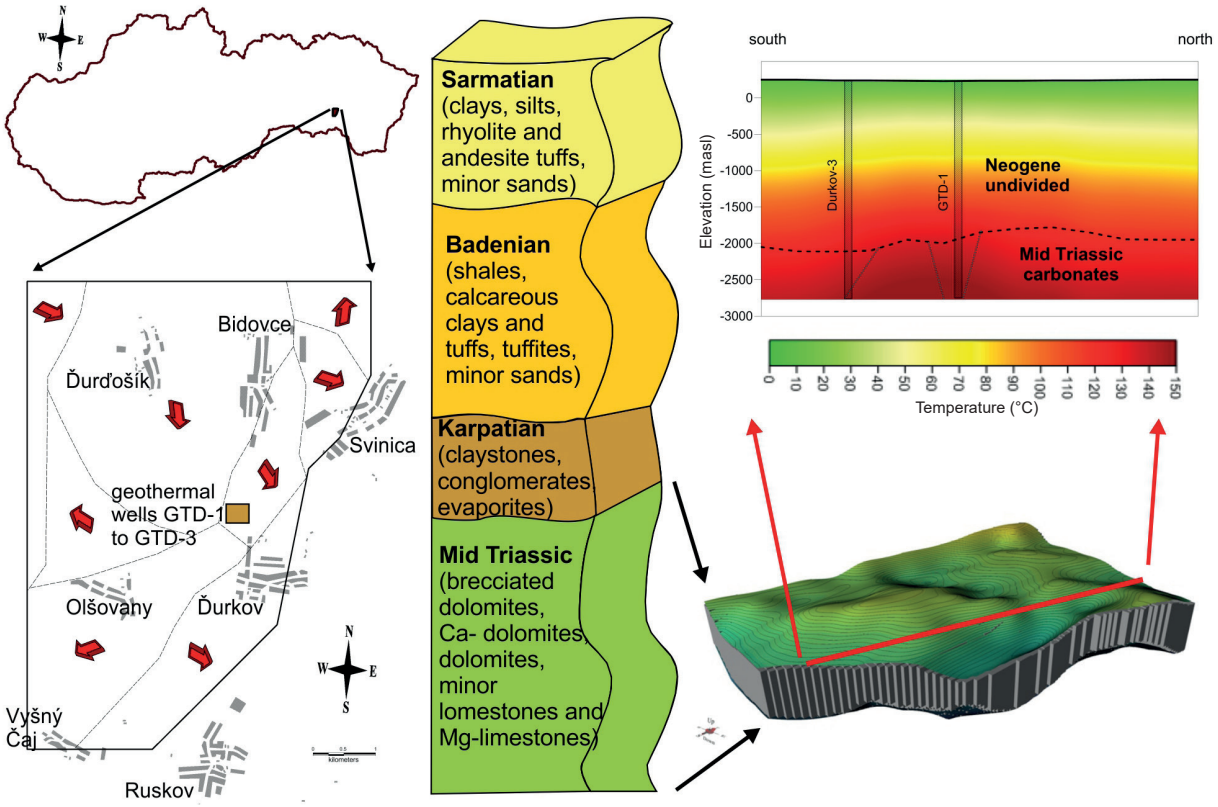

Fig. 4. 1. *Site definition of the Ďurkov Depression hydrogeothermal structure; tectonic segmentation with direction and slope of tectonic blocks; vertical profile and lithology, temperature profile and a reservoir body.*

system. As such, the 1st Law of Thermodynamics is adequate enough, whilst the resource and the system can easily be described according initial-state conditions; i.e. the temperature. However, resource production is an artificial aspect of geothermal energy utilization, far beyond a thermodynamic concept of a closed system. Indeed, multiple irreversibilities apply, the 2nd Law of Thermodynamics must be considered.

4.3.1 A concept of exergy

According to the 1st Law of Thermodynamics, the energy of the closed system at initial (natural) conditions is a conservative measure (1) well described along a balanced enthalpy flow (2). The latter neglects heat and work transfers (Ozgener et al., 2005, 2007):

$$\dot{Q}_{in} - \dot{Q}_{out} + \sum m_{in}.h_{in} = \dot{W}_{in} - \dot{W}_{out} + \sum m_{out}.h_{out} \quad (1)$$

$$\sum m_{in}.h_{in} = \sum m_{out}.h_{out} \quad (2)$$

where $\dot{Q}$ is heat transfer rate, is the mass flow, is the work rate, and h is the enthalpy; symbols "in" and "out" refer to system inlet/outlet conditions.

Under artificial production, the state of the system changes, and multiple irreversibilities apply as the entropy generates. Then, only a part of an energy can be sufficiently converted into a useful work – the exergy (DiPippo, 2005), also denoted as a thermodynamic quality (Lee, 1996). Unlike the energy, the specific exergy (3) is rather consumed or destroyed during a resource utilization due to entropy generation (Ozgener et al., 2005):

$$e = \left(h_{DP} - h_{RC}\right) - T_{RC}\left(s_{DP} - s_{RC}\right) \quad (3)$$

where e is the specific exergy, h is the enthalpy, T is the temperature, and s is the entropy; indexes "*DP*" and "*RC*" refer to a definition and reference point respectively.

A maximum thermodynamic quality (exergy) is achieved if the system transfers from definition to the dead-state p-T conditions. The latter corresponding to the triple-point (4):

$$e = h_{DP} - 273 s_{DP} \quad (4)$$

where e is the specific exergy, h is the enthalpy, and s is the entropy; index "*DP*" refers to a definition point.

Otherwise, pseudo-dead state conditions can be specified (Ozgener et al., 2006) variously; whether at reinjection or spill, a condenser etc. A definition point is typically defined to the borehole inlet or wellhead, as this takes an advantage in a fact that this is a first point where the resource can actually undergo a conversion process or can generate work (Lee, 2001).

4.3.2 A concept of specific exergy index classification

Geothermal resources (fields) tend to get subjected both for quantitative and qualitative analysis. In exergy concepts, the quantitative definition of thermodynamic quality relates to the specific exergy index – *SExI* (Lee, 1996, 2001) calculation. Instead of some arbitrary criteria, such as it is with the temperature, this is a normalized parameter (5) relating a maximum exergy of the system theoretically available, to the maximum exergy of a saturated steam at p = 90 Bar-abs and T = 303 °C with a triple point sink condition; i.e. e = 1,192 kJ.kg^{-1} (Lee, 2001):

$$SExI = \frac{h - 273.16s}{1192} \quad (5)$$

where *SExI* is the specific exergy index, and h and s refer to the geothermal resource enthalpy and entropy at a definition point.

To map thermodynamic quality, Lee (1996, 2001) introduced several limits: a *SExI* = 0.5 represents a thermodynamic quality of saturated steam at p = 0.1 MPa and T = 100 °C, whilst a *SExI* = 0.05 describes a thermodynamic quality of saturated water at T = 100 °C and p = 0.1 MPa. Thus, the *SExI* = 0.2 represents a limit for double-phase system at p = 2 MPa and h = 1,000 kJ.kg^{-1}. Under given criteria set, geothermal resources can be classified as:

a) low thermodynamic quality exergy; *SExI* < 0.05 (typically single-phase, water dominated geothermal fields)
b) moderate-low thermodynamic quality / exergy; 0.05 ≤ *SExI* < 0.2 (two-phase, water dominated geothermal fields)
c) moderate-high thermodynamic quality / exergy; 0.2 ≤ *SExI* < 0.5 (typically two-phase, vapour dominated geothermal fields)
d) high thermodynamic quality / exergy; *SExI* ≥ 0.5 (single phase dry steam, two-phase vapour dominated geothermal fields).

Along with numerical consideration, geothermal resources are frequently analyzed using Mollier's and Rant's diagrams, plotting enthalpy to entropy and entropy to the specific exergy of the resource respectively. Since introduction, the concept of exergetic (engineering) classification has been successfully applied in analyses of geothermal fields in Turkey (Etemoglu & Can, 2007), Poland (Barbacki, 2012), Japan (Jalilinasrabady & Itoi, 2013), Mexico (Ramajo et al., 2010) or in Slovakia (Fričovský et al., 2016a, b).

4.4 Geostatistical modelling

Geostatistics is a rapidly evolving scientific branch of applied statistics and mathematics that studies the spatial-temporal phenomena and thus extends the concept of traditional statistical methods of data processing in a spatial form. It was originally developed by George Matheron of Centre de Morphologie Mathématique in France for solving the problems of the ore reserve estimation in the mining industry but it is nowadays very popular not only in geology but also in many other areas of the natural science. Spatial data, in the framework of geosciences, exhibit some degree of spatial correlation, which is a function of the distance – the greater distance between samples, the lower

similarity between the data, but on the contrary, the higher is their variability (Matheron, 1963). The paper does not intend to present a deep review of geostatistics with all its algorithms and methods. A number of geostatistical books are available that document the principles, methods and techniques, including for instance Journel & Huijbregts (1978), Isaaks & Srivastava (1989), Clark & Harper (2000), Armstrong (1998), Goovaerts (1997), Webster & Oliver (2001), Wackernagel (2003), Chilès & Delfiner (2000), Olea (1999), Lantuéjoul (2002), Leuangthong et al. (2008), etc. Tonnes of notes, courses and papers have been published to study the topic. Since its definition in 1962 by George Matheron, initially developed for ore reserve estimation problems in the mining industry, geostatistics has evolved extremely, including many methods, techniques and approaches for spatial modelling of natural phenomenon in the Earth sciences. From mining, geostatistics has spread and has become an important methodology in many fields of application like petroleum industry, geology, climatology, agriculture, soil science, forestry etc. For these reasons, only a very brief introduction of geostatistics and very basic principles and terms will be given in this section.

Geostatistics provides a wide variety of tools to quantify and model the degree of spatial similarity and spatial variability. The aim of geostatistical methods for modelling of spatial variability is a random variable Z distributed in space and/or time. In geostatistical applications, a random variable is a function of spatial coordinates at any point of the studied area, in which each point $\mathbf{u}$ is determined by geographic (and/or time) coordinates in one, two or three-dimensional space; $\mathbf{u}$ = (X, Y, Z). Set of such random variables at each point $\mathbf{u}$ of the studied domain D represents a random function $Z(\mathbf{u})$. One realisation of a random function, or one realisation of each random variable in the space, consists of a set of values $z(\mathbf{u})$ called a regionalised variable (Matheron, 1971).

In geostatistical application, a random function $Z(\mathbf{u})$ can be expressed as the sum of two parts (Dowd, 2004):

1. A deterministic part $m(\mathbf{u})$, called *drift* or *trend*, represented by a deterministic function of location (linear, quadratic, etc.).
2. A stationary random function $R(\mathbf{u})$ with a constant mean that represents the deviation from the mean $m(\mathbf{x})$, so called residuals, and can be estimated by the standard techniques of stationary methods.

The above terms yield to the following expression of the random function $Z(\mathbf{u})$:

$$Z(\mathbf{u}) = R(\mathbf{u}) + \underbrace{m(\mathrm{u})}_{\mathrm{E}[Z(\mathbf{u})]}. \tag{6}$$

If we assume that the mean $m(\mathbf{u})$ is constant, then we have the basis for the geostatistical methods of overcoming the problems imposed by stationarity. A decision of stationarity of available data used for spatial modelling is necessary for all geostatistical modelling. However, as stated by Journel (1986), stationarity is a constitutive property of the random function and not an intrinsic property of the studied phenomenon and therefore a decision about stationarity is, in fact, a model itself.

4.4.1 Variogram

The variogram is the basic structural tool to model spatial continuity in geostatistical applications. It represents bivariate statistics, which express the variability of increments of the values z of random variables Z at points $\mathbf{u}$ separated by a vector $\mathbf{h}$. This direct variogram can be expressed as follows:

$$2\gamma_Z(\mathbf{h}) = \mathrm{E}\lfloor \{Z(\mathbf{u}) - Z(\mathbf{u}+\mathbf{h})\}^2 \rfloor = 2[\mathrm{C}_Z(0) - \mathrm{C}_Z(\mathbf{h})] \tag{7}$$

where $\mathrm{C}_Z(\mathbf{h})$ represents covariance between $Z(\mathbf{u})$ and $Z(\mathbf{u} + \mathbf{h})$ with constant mean m and $\mathrm{C}_Z(0) = \mathrm{Var}[Z(\mathbf{u})] = \sigma^2$ represents apriori variance of $Z(\mathbf{u})$. The variogram in (7) is valid only for stationary or weak stationary random processes (Matheron, 1971).

The expression (7) simply describes how the values of Z at two points $\mathbf{u}$ and $\mathbf{u} + \mathbf{h}$ become different as the separation vector $\mathbf{h}$ between pairs of points increases. Graphically, the variogram is a positive function increasing with $\mathbf{h}$ and it describes the change of the spatial variability of the studied features in the studied area for any distance and any direction of space (Armstrong, 1998).

The final model of the variogram describes the change of the spatial variability and, consequently, it is used in the geostatistical modelling. The main role of geostatistics is to make an estimation of the unknown value at unsampled locations.

4.4.2 Kriging

The geostatistical estimation procedure is called kriging, developed by George Matheron in 1963, and it is named in honour of Daniel G. Krige, following his university thesis. Nowadays, under kriging we understand "a collection of generalized linear regression techniques for minimizing an estimation variance" (Olea, 1991) that is used to estimate unknown values at unsampled locations using surrounding data $z(\mathbf{u}_\alpha)$. It is beyond the scope of the paper to present all different kriging techniques due to their wide variation. The paper presents the general model named universal kriging (abbr. UK). Matheron (1971) assumes that the mean in (1) can be written in a form of finite polynomial of order K, or trend, in practise of first or second order:

$$m(\mathbf{u}) = \sum_{k=0}^{K} a_k \mathbf{u}^k \tag{8}$$

Since kriging is a method of a linear regression, a weighted linear estimator at unsampled location $\mathbf{u}_\mathrm{o}$ in the stationary case where the mean m is known can be written as:

$$z^*(\mathbf{u}_\mathrm{o}) - m = \sum_{\alpha=1}^{n(\mathbf{u}_\mathrm{o})} \omega(\mathbf{u}_\alpha)\big(z(\mathbf{u}_\alpha) - m\big) \qquad \text{or shortly}$$

$$z^*_\mathrm{o} = \sum_{\alpha=1}^{n_\mathrm{o}} \omega_\alpha \underbrace{\big(z_\alpha - m\big)}_{\text{residuals } r_\alpha} \tag{9}$$

where ω_α are the weights assigned to the n_o data z_α within a search neighbourhood available for estimation. The estimation variance for universal kriging is given by (Dowd, 2004):

$$\sigma_e^2 = \mathrm{Var}\left[Z_o^* - Z_o\right] = 2\sum_{\alpha=1}^{n_o}\omega_\alpha\gamma_{\alpha o}^R - \sum_{\alpha=1}^{n_o}\sum_{\beta=1}^{n_o}\omega_\alpha\omega_\beta\gamma_{\alpha\beta}^R - 2\sum_{k=0}^{K}\lambda_k\left(\sum_{\alpha=1}^{n_o}\omega_\alpha\mathbf{u}_\alpha^k - \mathbf{u}_o^k\right) \quad (10)$$

with sample-to-sample variogram of residuals $\gamma_{\alpha\beta}^R$, sample-to-target variogram $\gamma_{\alpha o}^R$ and a set of Langrange multipliers λ_k for a given trend order K.

The weights ω_α in equation (9) are derived by minimizing of the estimation variance (10) and solving a kriging system of linear equation:

$$\begin{cases} \sum_{\beta=1}^{n_o}\omega_\beta\gamma_{\alpha\beta}^R + \sum_{k=0}^{K}\lambda_\alpha^k f_\alpha^k = \gamma_{\alpha o}^R \quad \forall\alpha \\ \sum_{\alpha=1}^{n_o}\omega_\alpha f_\alpha^R = f_o^k \quad \forall k \end{cases} \quad (11)$$

Associate kriging variance, independent of available data values, becomes:

$$\sigma_K^2 = \sum_{\alpha=1}^{n_o}\omega_\alpha\gamma_{\alpha o}^R - \sum_{k=0}^{K}\lambda_k\mathbf{u}_o^k. \quad (12)$$

4.4.3 Geostatistical simulations

The aim of kriging is to produce the best accurate estimation of the mean value of a random variable Z at an unsampled location $\mathbf{u}_o$, $E[Z(\mathbf{u}_o)]$ in the sense of the least-square method because of minimizing the local estimation variance σ_e^2. The spatial structure of the estimated values differs from that of the actual ones (de Fouquet, 1993). The map of kriged estimates is interpreted as a set of expectations of the random variables at all locations $\mathbf{u}_o$ and tends to smooth out the local variability of the data. That means that low values are overestimated whereas high values are underestimated. The smoothing effect of kriging is a serious disadvantage when trying to reproduce the extreme values. One important fact is that the smoothing effect of kriging depends on the data location – smoothing is smaller close to the data location and conversely. The final kriged map is therefore less variable than the data.

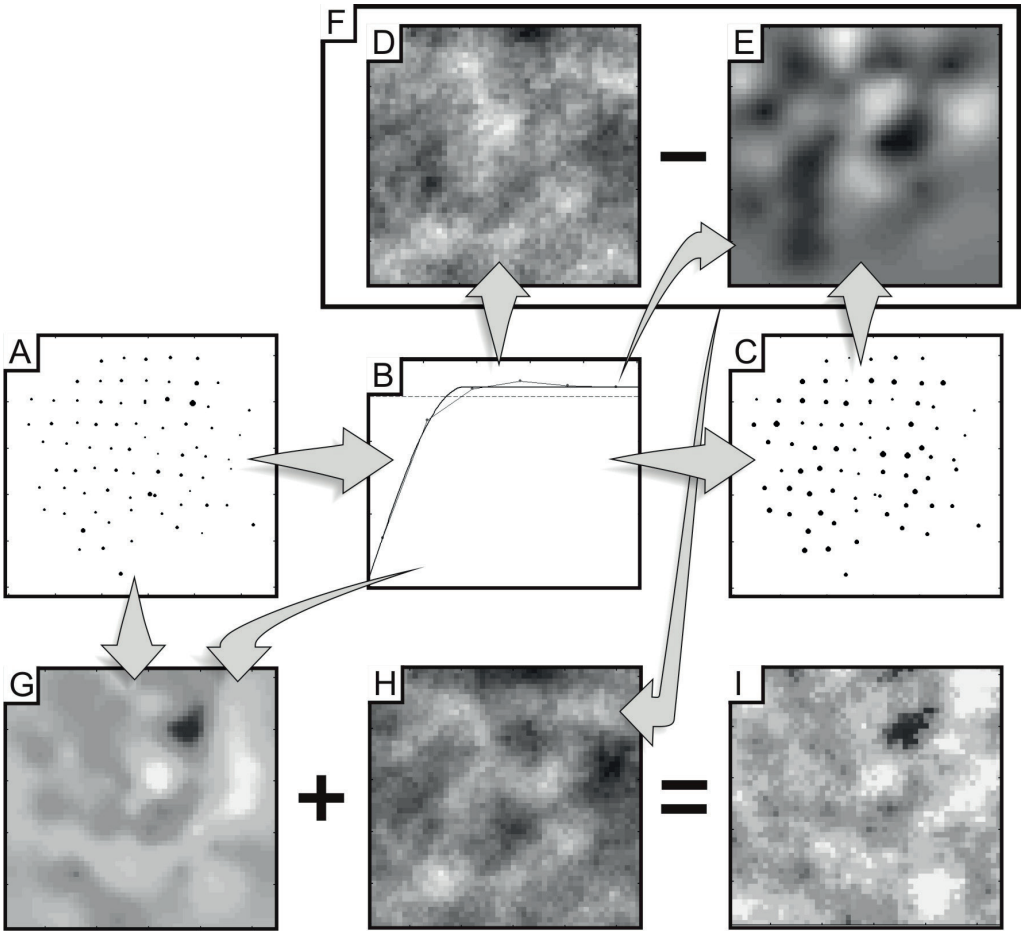

Fig. 4.2. *The values at sampling locations (A) are used to construct a variogram model (B). The model of variogram is used to simulate the values of the non-conditional simulation at the sample location to obtain $z_{NS}(\mathbf{x}_\alpha)$ (C) as well as on the grid nodes to get non-conditional simulation $Z_{NS}(\mathbf{x})$, which represents a reality with the same variability pattern as the sample values (D) Non-conditional simulation values at the sample locations $z_{NS}(\mathbf{x}_\alpha)$ are kriged on the grid nodes using the variogram model (B) to get a smooth estimation of the non-conditional simulation (E). Difference between non-conditional simulation and kriged non-conditional simulation gives a kriging error – a natural error, which appears when a reality is estimated from the samples (F). Conditional simulation (I) is finally built up by adding the simulated kriging error (H) to the kriging estimation of a regionalized variable (G) using the sample data (A) and the variogram model (B).*

Stochastic simulation produces the maps of realisations $z_s(\mathbf{u}_o)$ of a set of random variables $Z(\mathbf{u}_o)$ at all unsampled locations $\mathbf{u}_o$. The aim of the simulation is to randomly draw several realisations of the random function that reflect the variability of the sample values (data histogram and variogram). Each simulated realisation represents a possible version of reality coherent with the data values and a used model of variability as well. A simulation that does not honour the experimental data values is called non-conditional simulation (NS). There are many methods for generating a realisation of the non-conditional simulation (for example sequential methods, spectral methods, LU covariance matrix decomposition, turning bands, etc.). Each method has its own advantages and disadvantages, as may be seen for example in Chilès & Delfiner (1999) or Lantuéjoul (2002). In general, non-conditional simulation is one possible realisation of a random function that has the same variogram model as the one modelled from the sample data, but it is otherwise totally unrelated to them (Chilès & Delfiner, 1999). Non-conditional simulation is conditioned by kriging. Conditioning is a process by which we can pass from a non-conditional simulation Z_{NS} to a conditional simulation Z_{CS} that match the sample points $z(\mathbf{u}_\alpha)$ of random function $Z(\mathbf{u})$. Non-conditional and conditional simulations are independent, but with the same variogram model. Conditional simulation $Z_{CS}(\mathbf{u})$ is built by adding the kriging error $[Z(\mathbf{u}) - Z_K^*(\mathbf{u})]$ to the kriging estimation $Z_K^*(\mathbf{u})$. However, the kriging error is unknown because $Z(\mathbf{u})$ is not known. Therefore the kriging variance is replaced by non-conditional simulation of the kriging variance $[Z_{NS}(\mathbf{u}) - Z_{NS}^*(\mathbf{u})]$ where non-conditional simulation $Z_{NS}(\mathbf{u})$ is known on a simulated grid and is based on the variogram modelled from the sample data. Estimation of the non-conditional simulation $Z_{NS}^*(\mathbf{u})$ is based on kriging of the values of the non-conditional simulation at the sample locations $\mathbf{x}_\alpha$ using the same variogram model (Fig. 4.2).

A set of L independent and equal probable realisation of random function from conditional simulation constitutes a numerical model. Simulation post-processing and ranking of the realisations from the smallest realisation to the largest one enables us to construct an inverse distribution curve for any single cell of simulated grid, a group of cells or the entire area under consideration. The curve represents a probability, or risk curve.

The Turning Band (TB) algorithm was selected for simulation of the studied variables. It was the earliest algorithm for simulation of autocorrelated random processes in two or three dimensions (Deutch & Journel, 1998). The principle is to produce a non-conditional simulation that reflects the variogram but does not honour the input data. Independent one-dimensional realisations are first simulated along lines radiating from central points. Then, each point in 3D space is orthogonally projected into every line and the simulated values nearest to the projected points are averaged. The non-conditional simulation is then conditioned by kriging, which is used to interpolate the experimental error between data and non-conditional simulated values at the data points. The TB algorithm is suitable for all covariance models, does not assume Gaussian type model (Chilès & Delfiner, 1999) and it is great compromise between quality and computing time.

4.4.4 Input data and output geometry

Creation of final model began with a primary reservoir body dissection into 150 points regularly spaced of 500x500 m located on the top surface of the reservoir. Then, the reservoir was vertically divided into proportionally distributed 10 sublayers according to an overall reservoir thickness at given point on top reservoir surface. Thus, the studied hydrogeothermal reservoir Ďurkov was subdivided into 1,650 calculation points **u** in total.

Figs. 4.3 A and D show experimental histograms of both studied variables with used boundary conditions (or cut-offs):

1. Enthalpy h being equal or greater than 800 kJ.kg^{-1} ($h \geq 800$ kJ.kg^{-1}),
2. Specific exergy index *SExI* being equal or greater than 0.05 and 0.2 ($SExI \geq 0.05$, $SExI \geq 0.2$).

The experimental histogram of enthalpy shows approximately 10 % of its values above 800 kJ.kg^{-1} (166 calculated values of total 1,650) with their mean value 873 kJ.kg^{-1}. The histogram of specific exergy index shows almost 99 % its values above 0.05 (1,634 of 1,650) with the mean value 0.11 but it gets only 2 % values above 0.2 (34 of 1,650) with the mean value 0.215.

Fig. 4.4 shows spatial pattern and distribution for both studied variables. The spatial distributions look the same; differ only in scale. There is also a strong trend in the values increasing from the top to the bottom of the reservoir. That indicates a non-stationary phenomenon. As a matter of fact, the calculated variables of the specific enthalpy h and specific exergy index *SExI*, described in section 3, are function of temperature, which is, in fact, function of depth. Therefore, a non-stationary model was considered during spatial modelling phase under assumption of systematic increasing the values of studied variables in vertical direction. To build the non-stationary model, the first step consisted in modelling a trend function by means of the least square polynomial method fitting. Under assumption of stationarity in a horizontal plane XY; a linear model in form of $m(z) = a_0 + a_1 Z$ was fitted to obtain a stationary residual variables $R_h(\mathbf{u}_\alpha)$ and $R_{SExI}(\mathbf{u}_\alpha)$ The final residuals follow a normal distribution with zero means (Figs. 4.3 B and E, respectively).

Reservoir geometry is based on a multi-parametric model with inputs from borehole lithology, logging, seismic profiles and morphostructural maps (Vranovská et al., 1999b) and other hardcopy or grid data (Pachocká et al., 2010). Stationary thermodynamic data derivation succeeded geothermic calculations (temperature, heat flux, radiogenic heat production, etc).

The points with calculated variables under study served to model reservoir matrix prior processing in a refined 3D model with more than 1.4 million grid nodes with regular spacing 50x50x10 m for using of geostatistical simulations

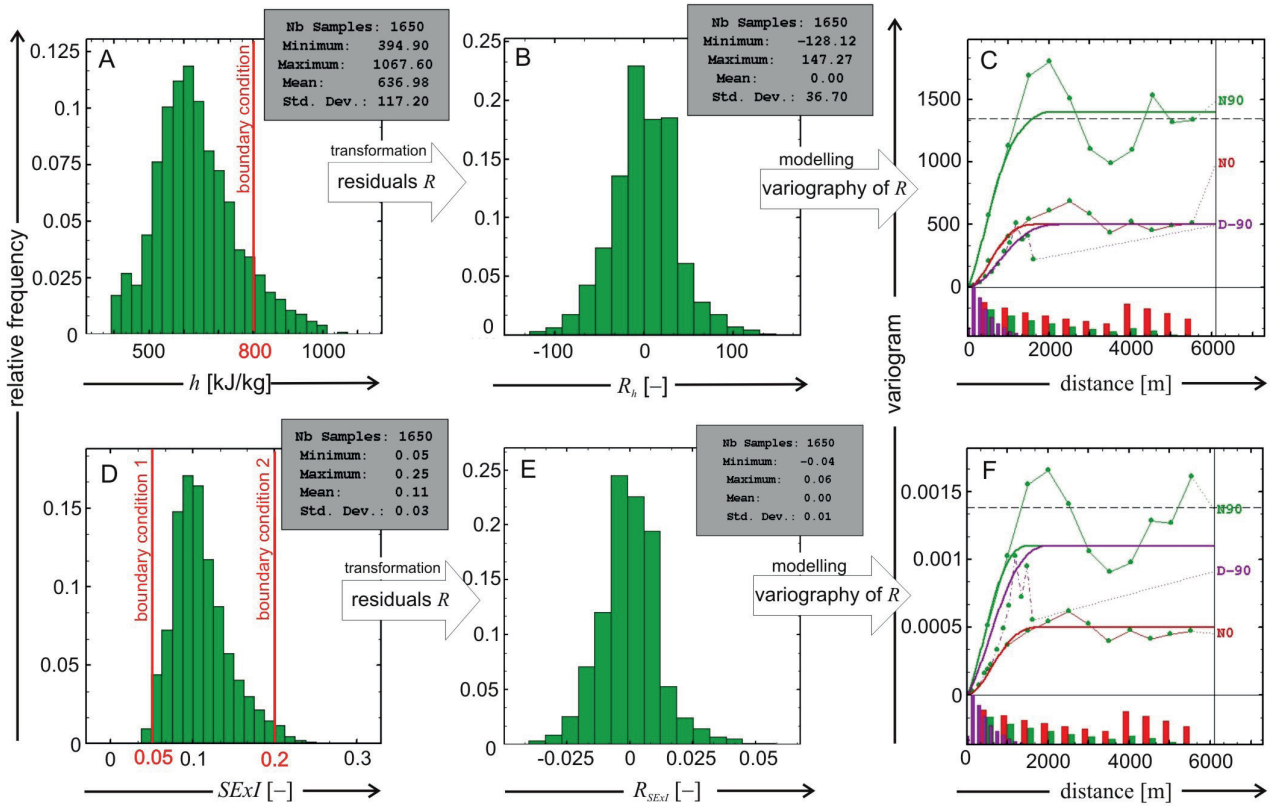

Fig. 4.3. *Experimental histogram of raw calculated data (A, D) their respective histograms of residuals (B, E) and final variogram models of residuals (C, F).*

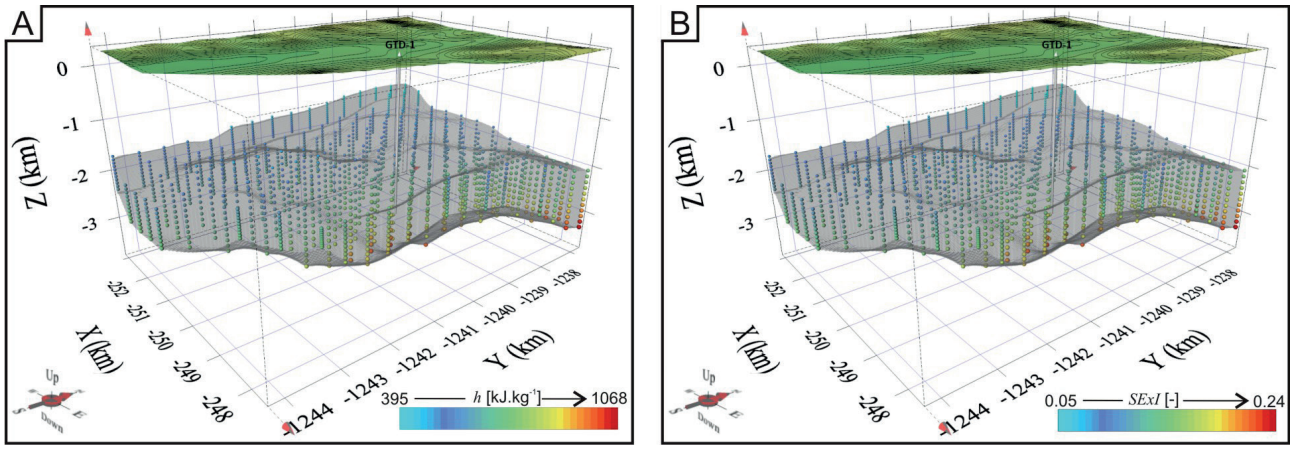

Fig. 4.4. *Spatial arrangement of 1,650 calculated sample points within 3D regular grid of Ďurkov reservoir shown in transparent grey. The sample points are coloured in accordance with the studied variable values for enthalpy (A) and specific exergy index (B).*

to create numerical models of the variables. It gives more than 35 milliards m^3 of total gross volume of the Ďurkov reservoir.

The experimental variograms were calculated for the residual variables: two experimental variograms in N-S and E-W directions in horizontal planes with lag distance 500 m in accordance with the sample spacing, and one experimental variogram in vertical direction. Nested basic structures of spatial variability were fitted to the directional experimental variogram to build variogram models. The final variogram models of calculated residuals are shown in Fig. 4.3 C for $R_h(\mathbf{u}_\alpha)$ and Fig. 4.3 F for $R_{SExI}(\mathbf{u}_\alpha)$. Both variogram models perfectly fit the directional experimental variograms with low nugget effect values and parabolic behaviour at the origins of models. They also exhibit a strong anisotropical pattern with apparent zonal anisotropy in horizontal plane prolonged in N-S direction, coincident with reservoir body and direction of main geological faults, and vertical direction toward the north, which is in accordance with stratified structure of the calculated variables under study. There is also presence of geometrical anisotropy between E-W and vertical directions and with higher continuity in E-W, which indicates the lowest continuity of studied variables in vertical direction, higher continuity in E-W direction and the highest continuity in N-S direction.

By adding the variogram models of residual variables to the linear trend model initialized at the trend modelling stage, the required non-stationary models are obtained, and subsequently used during geostatistical simulations.

4.5. Results

4.5.1 Geostatistical simulations

As stated previously, simulated grid consists of more than 1.4 million points on a 3D regular grid 50x50x10 m with total gross volume more than 35 milliards m^3. One hundred realisations in total were simulated by Turning Bands method using a given model variogram and search neighbourhood. Non-conditional simulations were conditioned by universal kriging due to using non-stationary structural model. The final numerical model consists of 100 simulated reservoir bodies filled by simulated values of studied variables specific enthalpy *h* and specific exergy index *SExI*.

Fig. 4.5 shows an example of reproduction of the statistical parameters of 1,650 input data and the same skewed shape of the input histogram for SExI shown in Fig. 4.4 D. In general, the individual simulations of the numerical model slightly exceeded experimental minimal and maximal values observed from the input data for both studied variables due to using non-stationary modelling approach. It is well know that the non-stationary approach often exceeds input data range mainly in extrapolation areas of studied domain. The mean values and standard deviation for the individual simulations of numerical model are well reproduced.

Fig. 4.6 shows the mean realisations for both studied variables, representing the spatial distribution of the variable values within the reservoir. The both models clearly show a reproduction of the spatial trend with the simulated values that increase with depth.

One hundred simulated values of the studied variables per each 3D grid node have been used to determine a value of parametric estimation either for enthalpy or specific exergy index in a 3D resolution. We used the given cut-off to detach a part of subpopulation estimated as under the criteria. This allowed delineation of local anomalies meeting a given criteria. Moreover, the cut-offs use also allowed probabilistic determination of distribution of selected variables and target values within the reservoir. Simulation post-processing consists in splitting each of 100 realisations into two parts – above and below a boundary condition (cut-off). On the grid node basis, post-processing continues with counting the number of times when the simulated values of each realisation exceed the boundary condition. This number is normalized by total number of realisations to obtain probability values ranging from 0 to 1. Figs. 4.7, C and D show such probability models. As can be seen, there is very tight transition in vertical direction among zero probability to exceed a given cut-off in the upper part of the reservoir and the very high probabilities at the lower part or at the bottommost parts of the reservoir for *SExI*.

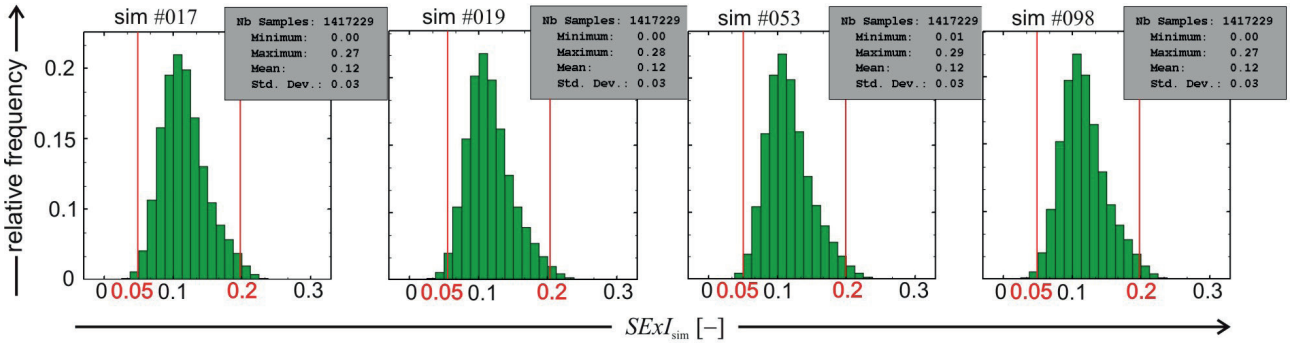

Fig. 4.5. *Experimental histograms of four randomly selected realisations of SExI simulation.*

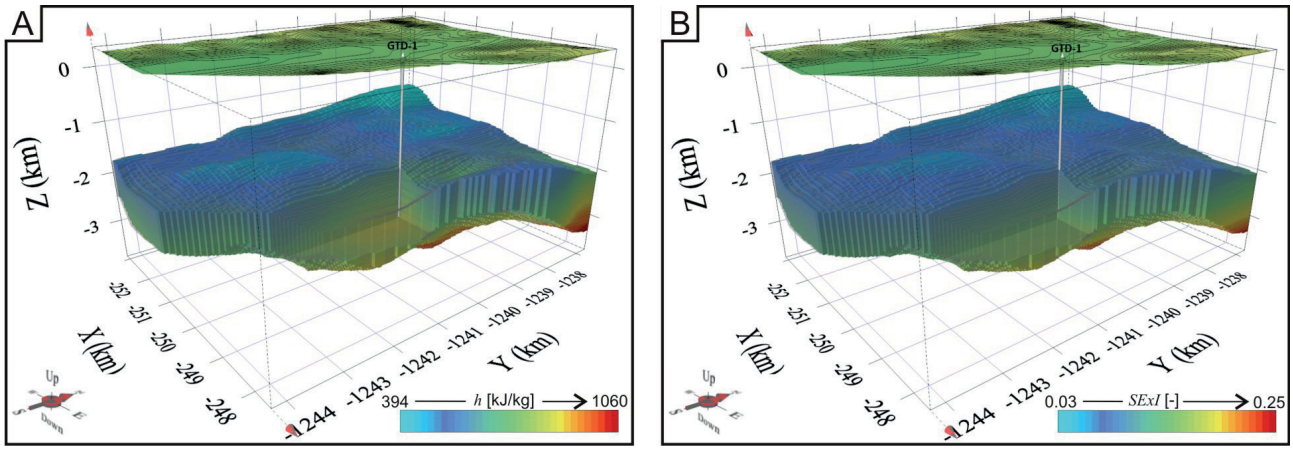

Fig. 4.6. *3D visualization of the mean realisations of the studied variables showing their spatial distribution within the Ďurkov reservoir.*

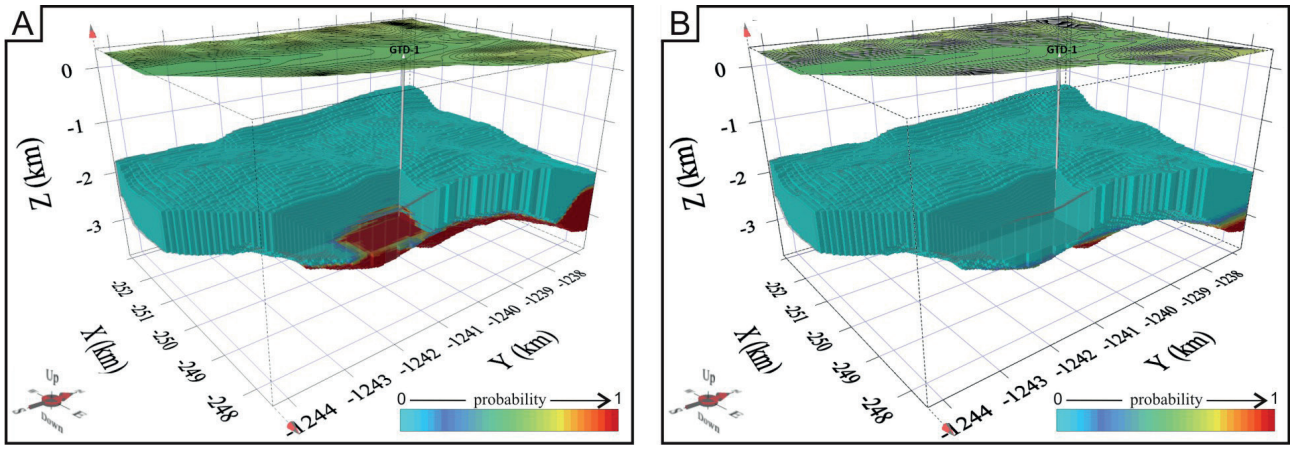

Fig. 4.7. *Probability models for* $h \geq 800$ kJ.kg^{-1} *(A) and* $SExI \geq 0.2$ *(B).*

In fact, there is approximately 5.8 milliards m^3 of volume within the reservoir where enthalpy exceed 800 kJ.kg^{-1} what gives only 16 % of total reservoir volume. Similarly, there is only 7 % (2.55 milliards m^3) of total reservoir volume with specific exergy index above 0.2.

Final probability models were used to construct the volumetrics risk curves as described in 4.3. The volumetrics curves for the studied variables are shown in Fig. 4.8. The final risk curves help to build different risk scenarios for the reservoir volume. For instance, there is only less than 10 % probability or less to get more than 609 Mm^3 of the reservoir volume with specific exergy index higher than 0.2. Or, there is less than 492 Mm^3 of reservoir volume with 90 % probability to get specific exergy index higher than 0.2. In other words, the reservoir volume will decrease with increasing probability to get values above a cut-off. Fig. 4.9 demonstrates the concept where we can clearly see that with increasing probability becomes the reservoir volume with $SExI \geq 0.2$ divided into two distinguishable zones.

4.5.2 Reservoir specific enthalpy

Most of studies on DDHS promote the system as of moderate to high temperature, according to local classification schemes (e.g. Fendek et al., 1999). Temperature (T_{gw}), total dissolved solids (M_{gw}) and calculated hydrostatic pressure (p_{gw}) were used to determine specific enthalpy in reservoir conditions; so that $h_{(z)} = f(T_{gw}, M_{gw}, p_{gw})$ where $T_{gw} = f(z)$, $M_{gw} = f(T_{gw})$ and $p_{gw} = f(z)$.

It is a clear SE trend observed for increase in specific enthalpy within the reservoir body as a function of depth and proximity to the Slanské vrchy Mts. The top of the reservoir extends in depths of 1,660 – 2,600 m, so that the reservoir enthalpy at a top varies h_{top} = 390 – 740 kJ.kg^{-1}. Approximately 50 % of the calculated enthalpy is less than h = 540 kJ.kg^{-1}. Towards the base at z = 1,960 – 4,000 m, the enthalpy fairly increases, i.e. h_{btm} = 440 – 1,060 kJ.kg^{-1}. As given by the model, a mean enthalpy at the base of the reservoir is h = 710 kJ.kg^{-1}. A most significant rise in enthalpy is estimated for the SE part of the system, where

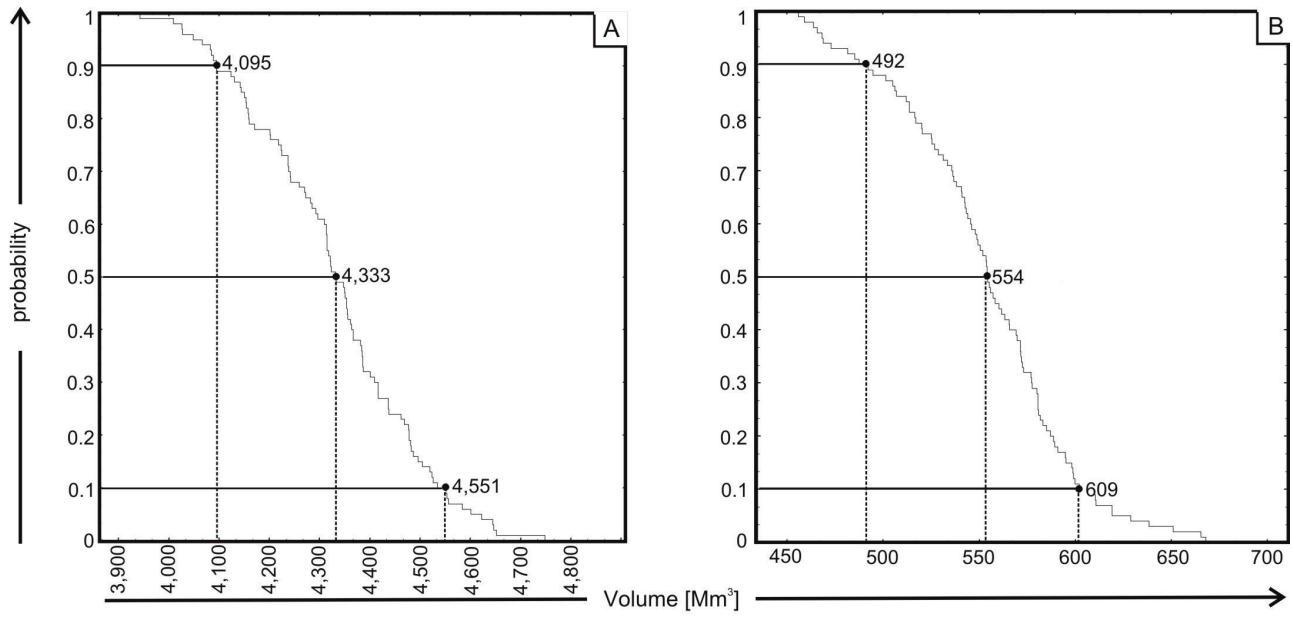

Fig. 4.8. *Final volume risk curves for* $h \geq 800$ kJ.kg^{-1} *(A) and* $SExI \geq 0.2$ *(B).*

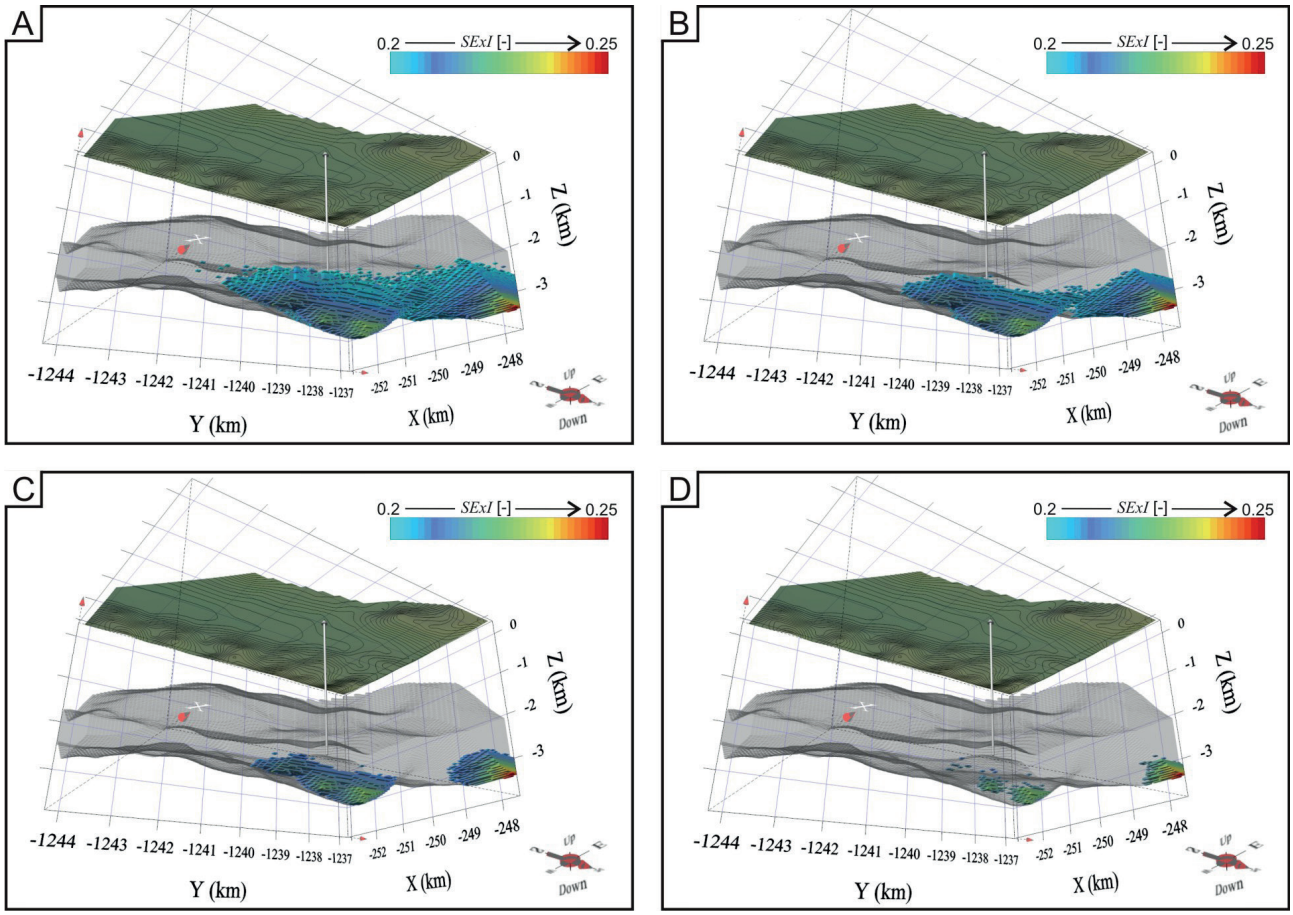

Fig. 4.9. *Probability models of SExI with extracting the non-zero probabilities (A), probabilities higher than 0.1 (B), 0.5 (C) and 0.9 (D).*

the gradient in enthalpy is δh_{res} = 200 – 260 kJ.kg^{-1}.km^{-1}. An overall thickness of the Middle Triassic carbonates in this part is assumed for Δz = 500 – 1,500 m.

Unlike general assumptions, only 16 % of the entire reservoir exceed the arbitrary given limit of h_{res} > 800 kJ.kg^{-1} criteria to distinguish between low and moderate (high) enthalpy geothermal waters. Distribution within the reservoir is uneven, skewed left. A zone of h_{res} > 800 kJ.kg^{-1} locates at the SE margin of the reservoir, in depths of z = 2,870 – 4,000 m below the surface. The zone of elevated, moderate (high) enthalpy, is most probably located east from the Ďurkov municipality. It corresponds to the tectonic block hit by geothermal wells GTD-1, GTD-2 and GTD-3. A vicinity to the neovolcanic Slanské vrchy Mts. and possible metamorphism plays a huge uncertainty to hydraulic properties in that zone though, increasing a risk of failure when tapping for geothermal water and deliverability. Instead of focusing to the E, we propose to delineate the prospective zone along a depressed block of carbonates running N and NE from geothermal wells.

4.5.3 Specific exergy index

By definition, the specific exergy index relates exergy of the given fluid described at a triple point conditions over a maximum exergy available, i.e. e = 1,192 kJ.kg^{-1}. Similar to specific enthalpy, we set the specific entropy; so that the $s = f(T_{gw}, M_{gw}, p)$. Thus, the specific entropy varies s_{top} = 1.2 – 2.1 kJ.kg^{-1}.K^{-1} for the top and increases to s_{btm} = 1.4 – 2.8 kJ.kg^{-1}.K^{-1} at a base of the reservoir. For the entire reservoir body, a mean specific entropy is estimated for s = 1.75 kJ.kg^{-1}.K^{-1}.

Quantitatively, the specific exergy index is calculated for *SExI* = 0.05 – 0.25, with a mean of *SExI* = 0.095 if the reservoir is taken as a solid body. This is strikingly different compared to other hydrogeothermal systems in the Western Carpathians. Based on local geometry and geothermics, a specific exergy index fairly increases between a top ($SExI_{top}$ = 0.04 – 0.06) and bottom ($SExI_{btm}$ = 0.1 – 0.25); so, a mean at a top and a base do (*SExI* = 0.08 and *SExI* = 0.14). A tendency of *SExI* to increase follows the trend of reservoir specific enthalpy; i.e. a clear trend with depth and a direction, the SE margin of the structure, is well expectable. Thus, for what is called the prospective zone in this paper, the specific exergy index interval reduces to *SExI* = 0.11 – 0.25 at depths of z = 2,870 – 4,000 m. However, *SExI* > 0.2 occupies a minimum depths of 3,100 m rather to the east. This part has not been documented yet, bearing a huge risk of failure when targeting to tap the geothermal resource there.

4.5.4 Thermodynamic quality classification

Under a given range of specific exergy index calculated, 99 % of the reservoir exceeds the *SExI* = 0.05 criterion to consider an associated resource as of moderate-low thermodynamic quality. Exception is the NW periphery of

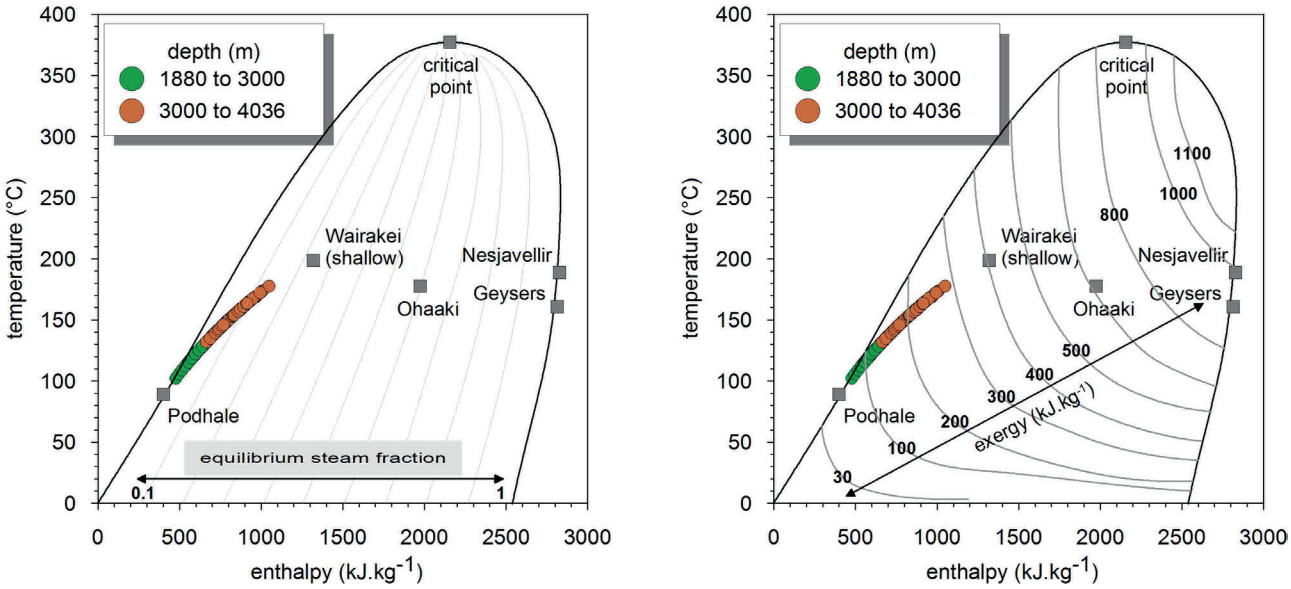

Fig. 4.10. The Ďurkov hydrogeothermal structure – "prospective zone"; T-h diagrams

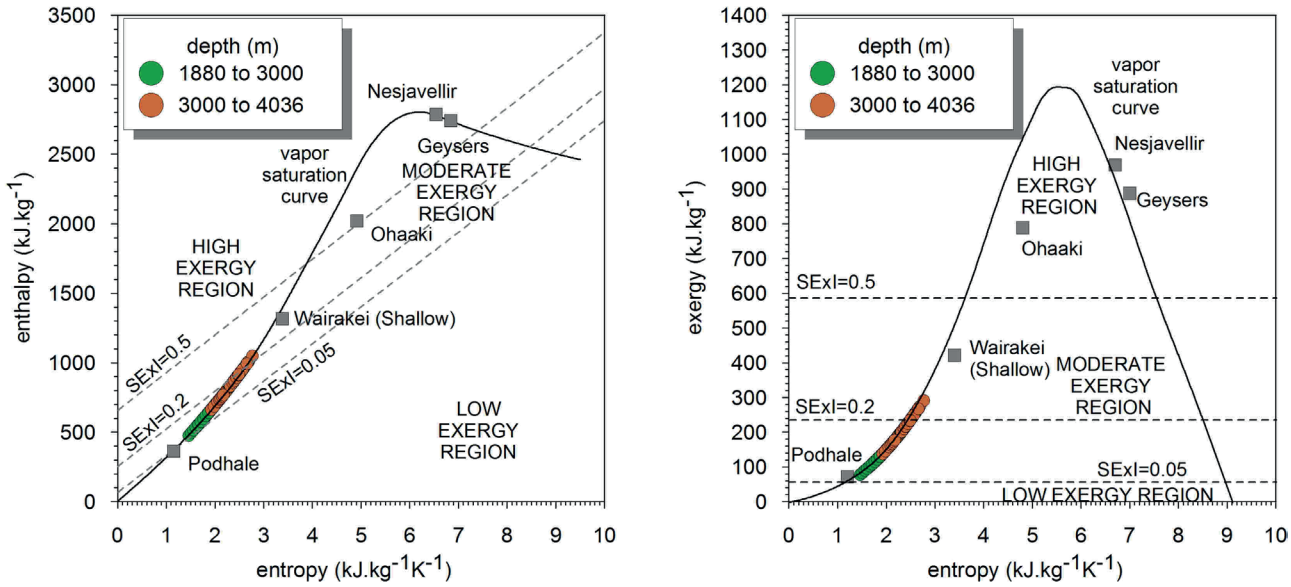

Figure 4.11. The Ďurkov hydrogeothermal structure – "prospective zone"; Mollier's (left) and Rant's (right) diagrams

the structure at depths of z = 1,660 – 1,780 m west from the municipality of Ďurďošík, where carbonates are fairly elevated (z_{top} = 1,600 – 1,800 m; z_{btm} = 1,800 – 4,000 m).

A second standard given by Lee (1996, 2001) recognizes moderate-high thermodynamic quality geothermal resources if *SExI* > 0.2. In geothermic conditions at the DDHS, approximately 7 % of the reservoir exceeds the level of specific exergy index only. Obviously, the zone of elevated thermodynamic quality correlates well to the zone of highest reservoir specific enthalpy, concentrated along E margin of the structure. When considering depths, zones, where moderate-high geothermal resource can be found with 90 % probability of success locates in depths of z = 3,100 – 3,900 m.

Indeed, a skepticism arises when evaluating the elevated thermodynamic quality, at least as implied by *SExI* calculation. A vicinity of neovolcanites triggers geothermic activity there. Meanwhile, an effect of metamorphism and reduction in permeability cannot be omitted. Thus, when considering an anomaly hunting / stacking approach (Cumming, 2009) for a future exploration of the entire geothermal structure, a focus on a tectonic block running NE between Ďurkov and Bidovce/Svinica towns is strictly recommended, as this has been sampled already. This should limit a risk of failure apparent where targeting for highest *specific enthalpy index* or enthalpy.

4.5.5 Thermodynamic quality mapping

To map thermodynamic quality of the geothermal resource associated with the Middle Triassic reservoir, we used state diagrams for enthalpy versus temperature (Fig. 4.10) and entropy versus enthalpy and exergy (Fig. 4.11); both plotting calculation results for a prospective zone of the reservoir only. This should be delineated as a part of the reservoir following a tectonic block hit by GTD-1 to GTD-3 wells in 1999 (Vranovská et al., 1999),

running N of the Ďurkov town and arching NE between the towns of Bidovce and Svinica (Fig. 4.1). Vertically, the zone is limited along a top and bottom of the reservoir. So, if we consider this part as elevated in geothermic and thermodynamic parameters, a rest of the reservoir is, consequently, of lower exergetic quality.

A plot of reservoir enthalpy to reservoir temperature shows only a minor equilibrated steam fraction up to X_S = 0.18, increasing with depth. In fact, recently unpublished sustainable reservoir management evaluation for the structure questions presence of a steam cap in the reservoir and so a possibility of a double phase at depths does. However, for a prospective zone, a resource specific exergy at a triple point conditions ranges $e = 90 – 290$ kJ.kg^{-1}. A reservoir out of the prospective zone does not reach the saturation curve at all. A difference between the DDHS and some geothermal systems worldwide is striking (Fig. 4.10), even if reservoir temperature is comparative. Indeed, with higher steam fraction at Wairakei ($X_S \approx 0.23$) or Ohaaki ($X_S \approx 0.6$), both record higher specific exergies; i.e. e = 400 kJ.kg^{-1} and e = 650 kJ.kg^{-1}, respectively; and are used for geothermal power production. It would, thus, be thermodynamically inefficient (if not impossible) to consider a direct or flashing power generation systems at the DDHS, even temperatures may imply some potential.

Evident is also the difference between the DDHS and selected geothermal fields on the Mollier's and Rant's plot (Fig. 4.11). Even within the prospective zone delineated by heat flux and temperature anomalies, when stacked, only a few percentages exceed a *SExI* = 0.2 (moderate-high exergy) line, although reservoir temperatures between the DDHS and, e.g. Ohaaki, are approximately the same. Rather is the system comparable to Podhale, Fuzhou, Tianjin or Balcova geothermal fields.

Thus, we recommend the system of DDHS to be classified as of moderate-low thermodynamic quality (moderate-low exergy).

4.6 Discussion and conclusions

The presented paper describes and applies geostatistical methodology of spatial modelling and risk assessment thermodynamic conditions of the Ďurkov hydrogeothermal structure in Slovakia. The DDHS is repeatedly reported as the most prospective geothermal system in the Western Carpathians. Three geothermal wells (GTD-1 to GTD-3) have been installed there in 1999 (Vranovská et al., 1999a, b; Beňovský et al., 2001) targeting the prospective tectonic block north from the Ďurkov village. The analysis and spatial modelling were based on calculated spatial data with enthalpy and specific exergy values in 1,650 points within the reservoir body. Geostatistical simulations were used to model the studied variables that are functions of temperature and depth under non-stationary assumption. For that reason, the turning bands simulation technique was chosen to create a 3D numerical model. Final numerical model constituted 100 simulated realisations that were used to delineate probable volume of the reservoir with the enthalpy above 800 kJ.kg^{-1} and specific exergy index above 0.05 and 0.5, respectively. The complete numerical model of the Ďurkov reservoir was used to construct probability risk curves for reservoir volume above the mentioned boundary conditions.

The Ďurkov structure includes about 16 % of the total reservoir volume with the enthalpy above 800 kJ.kg^{-1}. In accordance with the volume risk curve there is less than 13 % of the total volume with more than 10 % probability. For higher probabilities such as 50 % or 90 % there is only 5 % or 10 % reduction of the reservoir volume above the boundary condition.

The specific exergy index above 0.05 occupies almost the entire reservoir with negligible proportion below that values in NW part of the reservoir. On the other side, there is only 7 % of the total reservoir volume with specific exergy exceeding 0.2 in the east and north-east part of the Ďurkov reservoir, mostly with very low probabilities. Indeed, from the volume risk curve it can be conclude that for probability above 10% there is more than 75 % reduction of the original reservoir volume above 0.2 of the specific exergy index. Similarly, for median probability (50 %) there is another almost 10 % reduction of that volume and more than 20 % reduction for probability 90 % with clear separation of the volume into two distinguishable zones.

Thermodynamic conditions for the Ďurkov depression hydrogeothermal structure imply its similarity to several moderate enthalpy, liquid (water) dominated geothermal fields worldwide. Indeed, the Podhale (Barbacki, 2012), Tianjin (Axelsson & Dong, 1998), Fuzhou (Pang et al., 2015) or Balcova (Ozgener et al., 2006) systems produce a geothermal resource for large-scale utilization, such is the district heating or individual space heating in combination with agriculture and recreation. All are also classified of moderate-low or simply a moderate (*SExI* = 0.05 – 0.5) exergy. In fact, no project operates the Ďurkov Depression until now. Thermodynamically, the system is not adequate for power production, lacking a sufficient steam fraction. However, with a cumulative discharge of Q = 115 l.s^{-1} and thermal output of 28 MW$_t$ as proven over closed-looped pumping test, with GTD-1 serving as reinjection well (Vranovská et al., 1999b; Beňovský et al., 2001), utilization of a geothermal resource for geothermal district heating appears outright energetically and exergetically. The more is the fact accented with a town of Košice a 13 km to the west only, still served with coal and natural gas in district heating systems (Fričovský et al., 2013). Thus, instead of increasing a share of geothermal resources on a primary energy mix in the country; reducing energetic dependency of a state on foreign resources; CO_2 mitigation; and transition towards the sustainable development at least on a municipal scale, the geothermal resource is set stand-by, somewhat ignoring its potential.

The thermodynamic study on DDHS reservoir conditions has proven the site as of moderate-low thermodynamic quality. A low equilibrium steam fraction disqualifies other than direct use of the resource, proven by moderate *SExI* values above depths of 3,000 m. Beneath, a risk of failure when targeting that zone increases dramatically. Suitability of the resource for a large-scaled, district heating and cascaded projects is also proven along

a similarity of reservoir (and wellhead) conditions with geothermal fields worldwide.

References

Armstrong, M., 1998: Basic Linear Geostatistics. Springer, ISBN-10 3-540-61845-7.

Axelsson, G. & Dong, Z., 1998: The Tanggu geothermal reservoir (Tianjin, China), Geothermics, 27 (3), p. 271-294.

Barbacki, A., 2012: Classification of geothermal resources in Poland by exergy analysis – Comparative study, Renewable and Sustainable Energy Reviews, 16, p. 123-128.

Beňovský, V., Drozd, V., Halás, O., Vrana, O., & Vranovská, A., 2018: Investigation of the Ďurkov geothermal structure for utilization of geothermal energy, Bulletin d'Hydrogeologie, 17, p. 1-11.

Bodiš, D. & Vranovská, A., 2001: Genéza anomálneho obsahu arzénu v hydrogeotermálnej štruktúre Ďurkov [*Genesis of anomalous arsenic content in the* Ďurkov *hydrogeothermal structure*], Podzemná voda, XVIII (2), p. 123-136, in Slovak, English resume.

Bories, S.A. & Combarnous, M.A., 1973: Natural convection in a sloping porous layer, Journal of Fluid Mechanics, 57 (1), p. 63-79.

Bodvarsson, G.S., Benson, S.M. & Witherspoon, P.A., 1982: Theory of the development of geothermal systems charged by vertical faults, Journal of Geophysical Research, 87 (B11), p. 9317-9328.

Chilès, J. & Delfiner, P., 1999: Geostatistics: Modelling Spatial Uncertainty. John Wiley and Sons, Inc. New York. ISBN 0-471-08315-1.

Clark, I. & Harper, W.V., 2000: Practical Geostatistics 2000. Greyden Press, U.S.A. ISBN 0-9703317-0-3.

Cumming, W., 2009: Geothermal resource conceptual models using surface exploration data, Proceedings, 34th Workshop on Geothermal Reservoir Engineering, Stanford University, CA.

De Fouquet, C., 1993: Reminders on the conditioning kriging. In: Geostatistical simulations, p. 131-145. Edited by Armstrong M, Dowd, P., A. Kluwer Academic, Dordrecht.

Deutsch, C.V. & Journel, A.G., 1998: GSLIB Geostatistical Software Library. 2nd edition. Oxford University Press Inc. New York. ISBN 0-19-510015-8.

DiPippo, R., 2005: Geothermal power plants – principles, applications and case studies, Butterworth – Heinemann, New York.

Dowd, P.A., 2004: MINE5260 Non-Stationarity. MSc. in Mineral Resources and Environmental Geostatistics. University of Leeds, Leeds. 2004. U.K.

Etemoglu, A.B. & Can, M., 2007: Classification of geothermal resources in Turkey by exergy analysis, Renewable and Sustainable Energy Reviews, 11 (7), p. 1596-1606.

Fendek, M. & Fendeková, M., 2010: Country update of the Slovak Republic, Proceedings, World Geothermal Congress 2010, Bali, Indonesia.

Fendek, M. & Fendeková, M., 2015: Country update of the Slovak Republic, Proceedings, World Geothermal Congress 2015, Melbourne, Australia.

Fendek, M., Remšík, A. & Král, M., 1999: The nature of geothermal resources in Slovak Republic, Slovak Geological Magazine, 5 (1-2), p. 121-131.

Franko, O. & Melioris, L., 1999: Conditions for formation & extension of mineral and thermal waters in the Western Carpathians, Slovak Geological Magazine, 5 (1-2), p. 93-109.

Franko, O., Bodiš, D., Fendek, M. & Remšík, A., 1990: Outline of geothermal activity in Czecho-Slovakia, Geothermal Resource Council Transactions, 14 (I), p. 31-40.

Fričovský, B., Jacko Jr., S., Popovičová, M. & Tometz, L., 2013: Substitution approach in carbon dioxide emission reduction evaluation: case study on geothermal power station project plan Ďurkov (Košice Basin, Slovakia), International Journal of Environmental Science and Development, 4 (2), 2, p. 124-129.

Fričovský, B., Černák, R., Marcin, D. & Benková, K., 2016a: A first contribution on thermodynamic analysis and classification of geothermal resources of the Western Carpathians (an engineering approach), Slovak Geological Magazine, 16 (1), p. 94-117.

Fričovský, B., Černák, R., Marcin, D., Benková, K., Remšík, A. & Fendek, M., 2016b: Engineering approach in classification of geothermal resources of Slovakia (Western Carpathians), Proceedings, the 41st Stanford Geothermal Workshop on Reservoir Engineering, Stanford University, CA.

Fričovský B., Vizi, L., Gregor, M., Zlocha, M., Surový, M. & Černák, R., 2018: Thermodynamic Analysis and Quality Mapping of A Geothermal Resource at the Ďurkov Hydrogeothermal Structure, Košice Depression, Eastern Slovakia. Proceedings, 43rd Workshop on Geothermal Reservoir Engineering Stanford University, Stanford, CA.

Goovaerts, P., 1997: Geostatistics for Natural Resources Evaluation. Oxford University Press, Inc. 1997. London. ISBN 0-19-511538-4.

Halás, O., Drozd, V. & Vranovská, A., 1999: Investigation of Ďurkov geothermal structure in Košice Basin for geothermal energy utilization, Proceedings, XXIX IAH Congress: Hydrogeology and Land Use Management, Bratislava, Slovakia.

Hanano, M., 1998: A simple model of two-layered high-temperature liquid-dominated geothermal reservoir as a part of large-scale hydrothermal convection system, Transport in Porous Media, 33, p. 3-27.

Hanano, M. & Kajiwara, T., 1999: Permeability associated with natural convection in the Kakkonda Geothermal Reservoir, Geothermal Resources Council Transactions, 23, p. 351-360.

Isaaks, E.H. & Srivastava, R.M., 1989: An Introduction to Applied Geostatistics. Oxford University Press, Inc. New York. ISBN 0-19-505013-4.

Jalilinasrabady, S. & Itoi, R., 2013: Classification of geothermal energy resources in Japan applying exergy concept, International Journal of Energy Research, 37, p. 1842-1850.

Journel, A.G. & Huijbregts, C.J., 1978: Mining Geostatistics. Academic Press, Inc. London. ISBN 0-12-391050-1.

Journel, A.G., 1986: Geostatistics: Model and Tools for the Earth Sciences. Mathematical Geology, Vol. 18, No. 1, p. 110-130.

Kassoy, D.R. & Zebib, A., 1975: Variable viscosity effects on the onset of convection in porous media, The Physics of Fluids, 18 (12), p. 1649-1651.

Kukurugyová, M., Jablonský, G., Nalevanková, J. & Dzurňák, R., 2015: Production, profit and return of ORC-CHP geothermal power plant model at Ďurkov area, Slovakia, Proceedings, ISET 2015, Bratislava, Slovakia.

Kühn, M., Dobert, F. & Gessner, K., 2006: Numerical investigation of the effect of heterogeneous permeability distributions on free convection in the hydrothermal system at Mount Isa, Australia, Earth and Planetary Science Letters, 244, p. 655-671.

Lantuéjoul, Ch., 2002: Geostatistical Simulations. Models and Algorithms. Springer-Verlag Print, Berlin. ISBN 3-540-42202-1.

Lee, K.C., 1996: Classification of geothermal resources – an engineering approach, Proceedings, 21st Workshop on geothermal reservoir engineering, Stanford University, CA, USA.

Lee, K.C., 2001: Classification of geothermal resources by exergy, Geothermics, 30, p. 431-442.

Ledru, P. & Gillou-Frottier, L., 2010: Reservoir definition. In: Huenges, E. (Ed.): Geothermal Energy Systems. Exploration, Development and Utilization. Wiley-VCH Verlag, Weinheim, DE, p. 1-37.

Leuangthong, O., Khan, K.D. & Deutsch, C.V., 2008: Solved problem in geostatistics. John Wiley & Sons, Inc.. New Jersey. ISBN 978-0-470-17792-1.

Lipsey, L., Pluymaekers, M., Goldberg, T., van Oversteeg, K., Ghazaryan, L., Cloetingh, S. & van Wees J.-D., 2016: Numerical modelling of thermal convection in the Luttelgeest carbonate platform, the Nederlands, Geothermics, 64, p. 135-151.

Matheron, G., 1963: Principles of Geostatistics. Economical Geology, p. 1246-1266. Vol. 58.

Matheron, G., 1971: The theory of regionalized variables and its application. Les Cahiers du Centre de Morphologie Mathématique. École Nationale Supérieure des Mines Paris. Fontainebleau, Paris, France.

Moeck, I.S., 2014: Catalog of geothermal play types based on geologic controls, Geothermics, 37, p. 867-882.

Olea, R.A., 1991: Geostatistical Glossary and Multilingual Dictionary. Oxford University Press, Inc. ISBN 0-19-506689-9.

Olea, R.A., 1999: Geostatistics for Engineers and Earth Scientists. Kluwer Academic Publishers. ISBN 0-7923-8523-3.

Ozgener, L., Hepbasli, A. & Dincer, I., 2005: Energy and exergy analysis of geothermal district heating systems: an application, Building and Environment, 40, p. 1309-1322.

Ozgener, L., Hepbasli, A. & Dincer, I., 2006: Effects of reference state on the performance of energy and exergy evaluation of geothermal district heating system: A Balcova example, Building and Environment, 41, p. 699-709.

Ozgener, L., Hepbasli, A., Dincer, I. & Rosen, M.A., 2007: A key review on performance improvement aspects of geothermal district heating systems and applications, Renewable and Sustainable Energy Reviews, 11, p. 1675-1697.

Pachocká, K., Jacko, S. & Pachocki, M., 2010: 3D modeling of a geothermal reservoir in Eastern Slovakia, VDM Verlag Publ. Saarbrücken, 62 p.

Pang, Z., Luo, J., & Pang, J., 2015: Towards a new classification scheme of geothermal systems in China, Proceedings, World Geothermal Congress 2015, Melbourne, Australia.

Pasquale, V., Chiozzi, P. & Verdoya, M., 2013: Evidence for thermal convection in the deep carbonate aquifer of the eastern sector of the Po Plain, Italy, Tectonophysics, 594, p. 1-12.

Pereszlenyi, M., Pereszlenyiova, A. & Masaryk, P., 1999: Geological setting of the Košice Basin in relation to geothermal energy resources, Bulletin d'Hydrogéologie, 17, p. 1-8.

Rabinowicz, M., Sempéré, J-Ch. & Genthon, P., 1999: Thermal convection in a vertical permeable slot: Implications for hydrothermal circulation along mid-ocean ridges, Journal of Geophysical research, 104 (B12), p. 29275-29292.

Ramajo, H., Tritlla, J., Levresse, G., Tello-Hinojosa, E., Ramírez, G. & Pérez, H., 2010: New SExI tool to evaluate the evolution and anthropic disturbance in geothermal fields: the case of Los Azufres geothermal field, México, Revista Mexicana de Ciencias Geológicas, 27 (3), p. 520-529.

Ravenscroft, P.J., 1994: Conditional Simulation for Mining: Practical Implementation in an Industrial Environment. In Geostatistical Simulations. Armstrong, M.; Dowd, P.A.(Eds.), p. 79-89. Kluwer Academic Publishers. ISBN 0-7923-2732-2.

Rees, D.A.S. & Postelnicu, A., 2001: The onset of convection in an inclined anisotropic porous layer, International Journal of Heat and Mass Transfer, 44, p. 4127-4138.

Sclater, J.G. & Christie, P.A.F., 1980: Continental stretching: an explanation of the post Mid-Cretaceous subsidence of Central North Sea Basin, Journal of Geophysical Research, 85, p. 37111-3739.

Tóth, A.N., 2012: Heat losses in geothermal reservoir, Geosciences and Engineering, 1 (2), p. 321-327.

Vranovská, A., Bodiš, D. & Drozd, V., 1999: Zhodnotenie hydrogeotermálnej štruktúry Ďurkov na základe vrtov GTD-1,2 a 3 [*Evaluation of hydrogeothermal structure* Ďurkov *based on wells GTD-1,2 and 3*], Podzemná voda, V (2), p. 45-53, in Slovak, English resume.

Vranovská, A., Bondarenková, Z., Král, M. & Drozd, V., 1999: Košická kotlina - štruktúra Ďurkov - hydrogeotermálne zhodnotenie, vyhľadávací prieskum [*Košice Basin* – Ďurkov *structure, hydrogeothermal evaluation, exploratory survey*]. Manuscript – Final Report, Slovgeoterm / SGIDŠ, Bratislava, Slovak Republic. 90 p. In Slovak,

Vranovská, A., Beňovský, V., Drozd, V., Halás, O. & Váňa, O., 2000: Investigation for geothermal energy utilization in the town Košice, Slovak Republic, Proceedings, World Geothermal Congress 2000, Kyushu-Tohoku, Japan.

Vranovská, A., Bodiš, D., Šráček, O. & Ženišová, Z., 2015: Anomalous arsenic concentrations in the Ďurkov carbonate geothermal structure, eastern Slovakia, Environmental Earth Science, 73, p. 7103-7114.

Wackernagel, H., 2003: Multivariate Geostatistics. 3rd edition. Springer-Verlag Print, Berlin. ISBN 3-540-44142-5.

Wang, C.T. & Horne, R.N., 2000: Boiling flow in horizontal structure, Geothermics, 29, p. 759-772.

Webster, R. & Oliver, M.A., 2001: Geostatistics for Environmental Scientists. John Wiley & Sons, Inc. 2001. New York. ISBN 0-471-96553-7.